

Geometric approach to condensates in holographic QCD

Johannes Hirn,^{1,*} Nuria Rius,^{1,†} and Verónica Sanz^{2,‡}

¹IFIC, Departament de Física Teòrica, CSIC - Universitat de València,
Edifici d'Instituts de Paterna, Apt. Correus 22085, 46071 València, Spain

²Jefferson Laboratory of Physics, Harvard University, Cambridge, MA 02138, USA

Departamento de Física Teórica y del Cosmos, Universidad de Granada, Campus de Fuentenueva, 18071 Granada, Spain

An $SU(N_f) \times SU(N_f)$ Yang-Mills theory on an extra-dimensional interval is considered, with appropriate symmetry-breaking boundary conditions on the IR brane. UV-brane to UV-brane correlators at high energies are compared with the OPE of two-point functions of QCD quark currents. Condensates correspond to departure from AdS of the (different) metrics felt by vector and axial combinations, away from the UV brane. Their effect on hadronic observables is studied: the extracted condensates agree with the signs and orders of magnitude expected from QCD.

I. HOLOGRAPHIC QCD

Since the pioneering work of [1], some attention has been drawn to what is called *holographic QCD*. This was further studied using 5D models in [2, 3, 4]. Holographic QCD tries to answer the following question: *If it exists, how does the 5D dual of QCD look like?* The astonishing success of this bottom-up approach warrants a more detailed study of the qualities the dual should show, independently of a full-blown stringy set-up [5, 6, 7, 8, 9, 10, 11, 12, 13].

Our modus operandi consists of getting a handle on the known behavior of QCD and learning about the features the dual 5D model should have. At low energies, one possesses theoretical and experimental information concerning pion interactions. In the perturbative regime, the OPE of QCD, combined with the large- N_c expansion and the softness of some amplitudes are powerful theoretical guidelines for the 5D model's asymptotic behavior. In the intermediate region, experimental data on spin-1 resonances, like masses and widths, is available.

Here, we briefly outline the features of our model. Our starting point is the fact that gauge fields living in a 5D setup are supposed to have a 4D global symmetry dual. On the 4D side, QCD possesses a global $SU(N_f) \times SU(N_f)$ symmetry, whose spontaneous breaking gives rise to pions. The main ingredient of the 5D model is therefore the chiral symmetry of QCD promoted to a 5D gauge symmetry, as well as its breaking to the diagonal subgroup. A priori, the main difference between the approach of [2, 3] and that of [4], is the implementation of the symmetry-breaking. We discuss later how this influences physical predictions.

In our model we brought into play two ideas related to this breaking. First, boundary conditions (BCs) in the extra-dimension represent the spontaneous breaking by a 4D condensate of infinite dimension, before the AdS sin-

gularity has been smoothed out. Second, the gauge sector builds up the pion field: the Goldstone boson (GB) nature of the latter is thus ensured (protected to all orders by the 5D gauge symmetry [14]). These two inputs were enough to provide a massless pion with the right transformation properties: the model can be rewritten as a 4D lagrangian whose interactions explicitly obey chiral symmetry (for details, see [4]). This ensures that Green's function computed in the model will satisfy the Ward identities of chiral symmetry.

This picture of chiral symmetry breaking was just the entrée: in the massive sector, the two infinite towers of vector fields provided by a Kaluza-Klein decomposition have just the right symmetries to ensure softness of amplitudes at high energies. The reason behind is the underlying gauge structure which, from the 4D point of view, manifests itself in the form of clever sum rules between resonance couplings [4, 5]. Moreover, these two towers provide the partonic logarithm expected from asymptotic freedom, as a consequence of the asymptotic conformal invariance in the extra-dimension.

Furthermore, the lowest excitations could be identified as the observed ρ and a_1 mesons of QCD. Given as inputs the pion decay f_π constant and the rho mass M_ρ , the mass of the a_1 was predicted within the experimental range. Another conspicuous result of the 5D model is that the experimentally tested rho-meson dominance is an *automatic* property, whereas it was an *assumption* in 4D models for resonances. It is again a consequence of the extra-dimensional nature of the model, and manifests itself in 4D as the decrease of the couplings of the massive resonances to the pion. Since dominance of the ρ is satisfied within a few percent, and the soft high-energy behavior is ensured, the 5D models succeed in predicting the low energy constants of Chiral Perturbation Theory [15].

Such 5D models therefore match well to the low-energy predictions of QCD (which depend on chiral symmetry and lightest-meson dominance), as well as onto the HE

*Electronic address: johannes.hirn@ific.uv.es

†Electronic address: nuria@ific.uv.es

‡Electronic address: vsanz@ugr.es

partonic logarithms¹. In this work, we ask in addition to reproduce the analytic form of the first terms in the OPE as given in large- N_c QCD. Various Ansätze which perform this task for two-point functions can be constructed, however the 5D approach presents the following appealing features:

- There is no need to impose relations between (an infinite number of) constants to constrain the HE behavior: the 5D gauge symmetry takes care of that task.
- The condensates (power-corrections to the AdS metric) are input parameters in the 5D model, rather than derived quantities. The consequences of such deviations from conformality have computable effects on two-point and higher Green's functions [16, 17].

We provide the tools for studying the model in Section II, analyze the results in Section III and offer the conclusions in Section IV. Appendix A proves that our procedure respects covariance and locality and in Appendix B one can find the approximate dependence of hadronic observables on the condensates.

II. INCORPORATING CONDENSATES IN THE 5D MODEL

The simplest model presented in [4] was useful to illustrate a basic point: imposing the above-mentioned symmetries (AdS geometry and 5D gauge $SU(N_f)_L \times SU(N_f)_R \rightarrow SU(N_f)_V$) and adjusting two experimental inputs (f_π and M_ρ) was enough to obtain an agreement for low-energy quantities at the level expected for a model of large- N_c QCD at leading order.

The next step is to incorporate more features of QCD: the model of [4], defined on truncated AdS space with symmetry-breaking BCs lacks power corrections in the correlators, known to be present in QCD. Indeed, the OPE, for large euclidean momentum $Q^2 \equiv -q^2$ [18] should read, assuming factorization in the large- N_c

$$\begin{aligned} \Pi_{V,A}(-Q^2) &= -\frac{N_c}{12\pi^2} \left\{ \lambda + \log\left(\frac{Q^2}{\mu^2}\right) + \mathcal{O}(\alpha_s) \right\} \\ &+ \frac{1}{12\pi} \frac{\alpha_s \langle G_{\mu\nu} G^{\mu\nu} \rangle}{Q^4} + \left(\frac{-1}{11/7}\right) \frac{28 \pi \alpha_s \langle \bar{q}q \rangle^2}{9 Q^6} \\ &+ \mathcal{O}\left(\frac{1}{Q^8}\right), \end{aligned} \quad (2.1)$$

where λ is a subtraction constant. Note that dimension 4 and 6 condensates have quite different chiral properties: the former is chiral-invariant and therefore does not

contribute to $\Pi_V - \Pi_A$, whereas the latter contributes essentially to $\Pi_V - \Pi_A$ (2.1). This is why we will consider both of them. In [4] the $1/Q^{2d}$ pieces of the second line in (2.1) were absent, and numerical agreement for N_c was not imposed.

From the model building point of view, there are many ways to introduce the condensates but, at the end of the day, they are just modifications of the vector and axial wavefunctions located at a distance from the brane where the electroweak sector lives². Since the model of [4] already boasts a pion, there is no need for an extra spin-0 field: we therefore introduce all condensates as modifications of the metric. We will then be able to originate *both* axial and vector wavefunction modifications at once in a parametrically appealing fashion. This will have further consequences in the low-energy physics, since the modifications will be especially relevant there: we shall examine them in Section III.

A. Modifications of the metric and OPE

The extra dimension considered here is an interval. The two ends of the space are located at l_0 (the *UV brane*) and l_1 (the *IR brane*). With a purely AdS metric $w(z) = l_0/z$, the space-time interval then reads in conformal coordinates

$$ds^2 = w(z)^2 (\eta_{\mu\nu} dx^\mu dx^\nu - dz^2). \quad (2.2)$$

This reproduces the logarithm piece in (2.1), with only exponentially decaying corrections. Let us see how the power corrections of (2.1) can be generated. The high-energy expansion for the two point functions can be obtained by solving the following differential equation for a function $\varphi_X(z)$, ($X = V, A$)

$$\{Q^2 - \partial_z^2 - (\log w_X(z))' \partial_z\} \varphi_X(z) = 0, \quad (2.3)$$

where we have used the euclidean 4D momentum $Q^2 = -q^2 > 0$. The boundary conditions to be imposed on φ_X on the IR brane are the same as for the fields, respectively $\partial_z \varphi_V(Q, z)|_{z=l_1} = 0$ and $\varphi_A(Q, l_1) = 0$, while the value on the UV brane $\varphi_X(Q, l_0)$ is just a normalization. The two-point function is then obtained through [16, 17, 19, 20]

$$\Pi_X(-Q^2) = -\frac{2}{g_5^2} \frac{1}{Q^2} w_X(z) \left. \frac{\partial_z \varphi_X(Q, z)}{\varphi_X(Q, z)} \right|_{z=l_0} \quad (2.4)$$

With a purely AdS metric, $w(z) = l_0/z$, one obtains for $Q \gg 1/l_1$

$$\varphi(Q, z) \simeq Qz K_1(Qz), \quad (2.5)$$

¹ Note that this is realized with a fast-growing resonance spectrum: the mass of the n -th KK mode goes as n for $n \gg 1$, rather than \sqrt{n} obtained from linear Regge trajectories.

² In [2, 3], couplings of spin-1 fields to a scalar sector were responsible of modifying the axial wavefunction *only*. No $1/Q^6$ were generated in the vector two-point function, in disagreement with (2.1). Neither were $1/Q^4$ terms included, also in contradiction with (2.1).

which reproduces the log piece in (2.1) with the matching

$$N_c = \frac{12\pi^2 l_0}{g_5^2}. \quad (2.6)$$

Assume now that the metrics near the UV take the form

$$\begin{aligned} \frac{z}{l_0} w_{V,A}(z) &\simeq 1 + \frac{9\pi^2}{4N_c} \langle \mathcal{O}_4 \rangle (z - l_0)^4 \\ &+ \frac{5\pi^2}{16N_c} \left(\frac{-1}{11/7} \right) \langle \mathcal{O}_6 \rangle (z - l_0)^6 \\ &+ \mathcal{O} \left((z - l_0)^8 \right), \end{aligned} \quad (2.7)$$

where we have already adopted a convenient name for the coefficients $\langle \mathcal{O}_4 \rangle, \langle \mathcal{O}_6 \rangle$. With the metric (2.7), one solves the differential equation (2.3) to obtain $\Pi_{V,A}$ via (2.4)

$$\begin{aligned} \Pi_{V,A}(-Q^2) &= -\frac{N_c}{12\pi^2} \left(\log \left(\frac{Q^2}{\mu^2} \right) + \lambda(\mu) \right) + \frac{\langle \mathcal{O}_4 \rangle}{Q^4} \\ &+ \left(\frac{-1}{11/7} \right) \frac{\langle \mathcal{O}_6 \rangle}{Q^6} + \mathcal{O} \left(\frac{1}{Q^8} \right). \end{aligned} \quad (2.8)$$

Deviations from conformality with a given power of z^{2d} in the metric (2.7) yield a power of $1/Q^{2d}$ in the two-point function, with a computable coefficient. Note that $\mathcal{O}(\alpha_s)$ contributions in (2.1) can be accounted as inverse powers of $\log z$ in the metric³. However, we restrict our attention to the condensates here.

In the following, we will use the particular functional form

$$w_X(z) = \frac{l_0}{z} e^{\frac{9\pi^2}{4N_c} \langle \mathcal{O}_4 \rangle (z - l_0)^4 + \frac{5\pi^2}{16N_c} \left(\frac{-1}{11/7} \right) \langle \mathcal{O}_6 \rangle (z - l_0)^6} \quad (2.9)$$

for which a given power of z^{2d} in (2.7) yields *exactly* a power of $1/Q^{2d}$: only when multiplying (2.9) by $\exp \left(\frac{12\pi^2}{N_c} \frac{\Gamma(d+1/2)}{\sqrt{\pi} d^2 \Gamma(d)^3} \langle \mathcal{O}_{2d} \rangle (z - l_0)^{2d} \right)$ is a term $\langle \mathcal{O}_{2d} \rangle / Q^{2d}$ generated in (2.8).

Representing deviations from conformality as deviations of the metric from AdS provides a basis to enforce the OPE of QCD term by term. Including the lowest dimension condensates should be sufficient. Indeed, one would naively expect a condensate of dimension $2d$ to be of order the confinement scale to the appropriate power, i.e. $\Lambda_{\text{QCD}}^{2d}$, and to be proportional to N_c in the large- N_c limit. Trading Λ_{QCD} for the scale $1/l_1$ in the 5D model which induces the mass gap, one thus expects

$$\langle \mathcal{O}_{2d} \rangle \sim \frac{N_c}{l_1^{2d}}, \quad (2.10)$$

³ We thank Ami Katz for pointing out this fact to us.

or smaller. Plugging this back into (2.9), one sees that the deviations of the metric are of order one for the dimension 4 and 6 condensates, but decrease quite fast with d , as $\frac{\Gamma(d+1/2)}{d^2 \Gamma(d)^3}$. Comparing our model to data in Section III, we will indeed extract values for condensates that are within the expected range of (2.10) and of QCD phenomenological analyses, confirming the consistency of the whole approach.

Note that, since it is an order parameter, the dimension-6 condensate generates a power correction to $\Pi_V - \Pi_A$, implying that there are only two vanishing Weinberg sum rules. To reproduce this, it is necessary that the wavefunctions of the vector and axial fields *feel* a different metric. Otherwise one would have $\langle \mathcal{O}_6 \rangle_A = \langle \mathcal{O}_6 \rangle_V$ in (2.8), in contradiction with the QCD OPE Eq.(2.1). We explain how this essential point is achieved in the next Section and Appendix A.

B. Definition of the model

The model is defined by an $SU(N_f) \times SU(N_f)$ YM lagrangian in an extra dimension. We limit ourselves to terms involving two derivatives. Denoting by $w_{V,A}(z)$ respectively the warp factors that will be identified later as the metrics felt by the vector and axial fields, we start from the action

$$\begin{aligned} \mathcal{S}_{\text{YM}} &= -\frac{1}{4g_5^2} \int d^4x \int_{l_0}^{l_1} dz \eta^{MN} \eta^{ST} \\ &\times \left\{ \frac{w_V(z) + w_A(z)}{2} \langle L_{MS} L_{NT} + R_{MS} R_{NT} \rangle \right. \\ &\left. + (w_V(z) - w_A(z)) \langle L_{MS} \Omega^\dagger R_{NT} \Omega \rangle \right\}, \end{aligned} \quad (2.11)$$

where the capital letter index runs over the five dimensions. The last term in (2.11) summarizes the low-energy effects of couplings to other fields, and will ultimately be responsible for the vector and axial metric being different. It involves a unitary auxiliary field $\Omega(x^\mu, z)$, transforming as a bifundamental under the gauge groups. This spurious field is eliminated by imposing the constraint $D_5 \Omega = 0$.

Note that a term of a similar form, and with similar effects could be written down in the model of [2, 3], using (instead of the spurion Ω) a bulk scalar Φ . Yet, since Φ is dimensionful, this term could only appear at higher orders, presumably suppressed by a large scale. In our subsequent fit to experimental data, we shall however find that the order of magnitude of this term is in agreement with our including it at leading order, i.e. as a deformation of the metric rather than as a higher-order term. This is directly related to the above estimate of N_c/l_1^{2d} as the size of the condensates. Quite the opposite from being a large scale, $1/l_1$ is the only scale in the theory: modifications of the metric are of order one (for the lowest dimension condensates).

Another ingredient in [4], responsible for the presence of a well-defined pion in the spectrum, consists of the

choice of BCs. At the IR boundary $z = l_1$: $L_\mu - R_\mu = 0$ and $L_{5\mu} + R_{5\mu} = 0$. At the UV boundary, classical configurations serve as sources $\ell_\mu(x), r_\mu(x)$ for the analogue of the QCD quark currents, i.e. $L_\mu(x, z = l_0) = \ell_\mu(x)$ and $R_\mu(x, z = l_0) = r_\mu(x)$. Since the spurion satisfies $D_5\Omega = 0$, we need only one boundary condition, and we choose $D_\mu\Omega(x, z = l_1) = 0$. As shown by a covariant treatment (Appendix A), the action (2.11) is equivalent to writing a lagrangian in terms of vector and axial field strengths, but with different metrics, respectively w_V and w_A .

C. Sum rules

In [4], four sum rules involving 4D resonances couplings emerged as a consequence of the underlying 5D gauge structure. Three of them, together with the relations

$$L_3 = -3L_2 = -6L_1, \quad (2.12)$$

ensured the unsubtracted dispersion relation for the vector form factor, as well as the once-subtracted dispersion relation for GB forward elastic scattering amplitudes. These sum rules still hold with the present modifications of the metric, the same consequences for the behavior of the amplitudes therefore follow.

The only sum rule that does not hold anymore when $w_A \neq w_V$ is the one related to the KSFR II ratio: we derive $f_\pi^2 / (\sum_n g_{V_n}^2 M_{V_n}^2) > 3$ as long as $w_V(z) - w_A(z) < 0$ (as expected in order to reproduce the result of [21] that $\Pi_V - \Pi_A < 0$). Since this sum rule was the only one *not* related to any high-energy constraint, this has no theoretical consequences. From the phenomenological point of view, it is known that a KSFR II ratio of two is favored, but in a model, this depends on the predicted values of f_π and M_ρ : the agreement is best judged on the observable $\Gamma_{\rho \rightarrow \pi\pi}$, see Table I.

On the other hand, the case $w_A \neq w_V$ gives rise to a new sum rule (derived using the completeness relations for the wave-functions of the axial KK modes)

$$\sum_{n=1}^{\infty} f_{A_n} (f_{A_n} + 2\sqrt{2}\alpha_{A_n}) = 4(L_9 + L_{10}), \quad (2.13)$$

in the notation of [4]. Each term in the left-hand side vanishes separately when $w_V = w_A$. Due to this sum rule, the axial form factor $G_A(q^2)$ satisfies an unsubtracted dispersion relation

$$G_A(q^2) = \sum_{n=1}^{\infty} f_{A_n} (f_{A_n} + 2\sqrt{2}\alpha_{A_n}) \frac{M_{A_n}^2}{M_{A_n}^2 - q^2}. \quad (2.14)$$

The modification $w_V \neq w_A$ implies immediately $L_9 + L_{10} \neq 0$, and in general $f_{A_n} + 2\sqrt{2}\alpha_{A_n} \neq 0$ (at least for some n). In addition, since the width $\Gamma_{a_1 \rightarrow \pi\gamma}$ is proportional to $(f_{A_1} + 2\sqrt{2}\alpha_{A_1})^2$ [22, 23], this is accompanied

in general by a non-zero decay of a_1 into $\pi\gamma$. For a discussion of the numerical values of these two quantities, see Appendix B.

D. Quark masses

The electroweak interactions live on the UV brane, which we will therefore also call the EW brane. These interactions induce masses for the quarks via the Higgs mechanism of the SM. This in turn breaks the chiral symmetry explicitly: since we are only modelling QCD, and not electroweak symmetry breaking, we simply consider hard quark masses. In the present model as in χ PT [24], such quark masses can be introduced via a spurious field $\chi(x)$ transforming as a bifundamental under the chiral $SU(N_f) \times SU(N_f)$ symmetry of our 4D world. In our model, this translates as a 4D bifundamental under a subset of the 5D $SU(N_f) \times SU(N_f)$, namely the one acting on the EW brane. With such an object, one can write down the following term on the UV boundary

$$\frac{f_\pi^2}{4} \langle \chi(x) \Omega^\dagger(x, l_0) \rangle + \text{h.c.}, \quad (2.15)$$

where one has to keep in mind that χ should be counted as equivalent to an object containing two derivatives, and must be set equal to the quark mass matrix times a constant B_0 (of dimension one).

The key point is then to use the consequences of the constraint $D_5\Omega = 0$ and the rewritings of Appendix A, which lead to $\Omega(x, l_0) = U(x)$, i.e. the GB matrix. We thus recover the χ PT term $f_\pi^2/4 \langle \chi U^\dagger \rangle$. From this it follows, strictly as in χ PT, that B_0 gives a measure of the quark condensate at tree level, according to [24]

$$\langle \bar{q}q \rangle = -f_\pi^2 B_0. \quad (2.16)$$

As in χ PT again, the term (2.15) also induces a mass for the GBs, which become pseudo-Goldstone bosons. Disregarding isospin breaking effects, this reads [24]

$$M_\pi^2 = B_0(m_u + m_d). \quad (2.17)$$

We will use the value $M_\pi = 135$ MeV in the analysis of Section III.

To summarize the situation in the present model, we see that explicit symmetry breaking by quark masses, which is given by a 4D lagrangian on the EW brane, works exactly as in 4D χ PT, provided one realizes the equivalence between $\Omega(x, l_0)$ and $U(x)$. This is also true of the higher orders.

III. NUMERICAL RESULTS WITH CONDENSATES

Once the model has been rewritten in terms of vector and axial combinations as in Appendix A, one can

proceed following the method of [4] to compute masses, couplings and decay widths of the pion, rho and a_1 . In addition to f_π, M_ρ, M_{a_1} , the following couplings can be easily tested: the coupling of the ρ to the vector current is tested in $\Gamma_{\rho \rightarrow ee}$, its coupling to two pions in $\Gamma_{\rho \rightarrow \pi\pi}$, and the couplings of the a_1 to the axial current in $\Gamma_{\tau \rightarrow a_1 \nu_\tau}$, which we compare to the experimental $\Gamma_{\tau \rightarrow 3\pi \nu_\tau}$. We thus fit data by minimizing the RMS error on the six quantities $f_\pi, M_\rho, M_{a_1}, \Gamma_{\rho \rightarrow ee}^{1/4}, \Gamma_{\rho \rightarrow \pi\pi}^{1/4}, \Gamma_{\tau \rightarrow a_1 \nu_\tau}^{1/4}$, with respect to their central values provided in [25].

We performed a numerical analysis of these quantities in terms of the condensates and find that the favored region in parameter space is consistent with the estimate $|\langle \mathcal{O}_{2d} \rangle| \lesssim N_c l_1^{-2d}$. One can then in turn predict the values of the low-energy constants L_i appearing in the low-energy expansion of the model.

In the favored region, the approximate expression at linear order in the condensates are accurate within a few percents for f_π, M_ρ, M_{a_1} and the L_i constants. We present these expressions in Appendix B.

A. Strategy and results

In Ref.[4], we followed an approach centered on low-energies: we imposed $f_\pi = 87$ MeV (in the chiral limit) and $M_\rho = 776$ MeV. This led to agreement within the expected range ($1/N_c$ corrections) for low energy quantities: the mass of the a_1 , decays of the ρ , and allowed to predict the low-energy constants of χ PT. On the other hand, this exhausted the free parameters of the model, and yielded a mismatch in the OPE: the coefficient of the logarithm led to $N_c = 4.3$ in Eq.(2.6) for the chiral limit.

Another way to see this is that a pure AdS model with $N_c = 3$ but without condensates naturally underpredicts f_π and the χ PT low-energy constants (Table I). This mismatch is the evidence that, in order to interpolate between very high and very low energies with better precision, another ingredient is needed: the condensates. In the present paper, we start by imposing $N_c = 3$, as in [2, 3]. In the pure AdS case, this leaves us with one free parameter l_1 , which we adjust to minimize the RMS error on the six observables $\sqrt{\sum (\delta O/O)^2 / n}$, where n is the number of observables minus parameters ($n = 5$). The best fit is obtained for $l_1 \simeq 3.1 \text{ GeV}^{-1}$, yielding an RMS error of 12.5%. This is our input Set A, which constitutes a benchmark result without condensates: the outputs can be read in Table I.

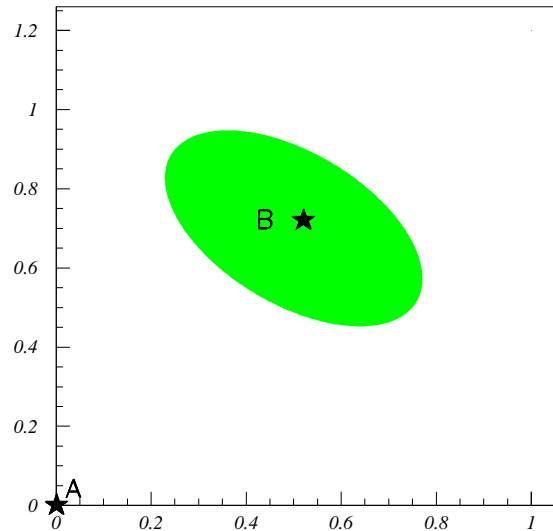


FIG. 1: Sketch of the favored parameter space: the x -axis represents $\langle \mathcal{O}_4 \rangle$ in units of 10^{-3} GeV^4 and the y -axis represents $\langle \mathcal{O}_6 \rangle$ in units of 10^{-3} GeV^6 .

The next step is to include the condensates. Dimensional analysis showed that only the dimension 4 and 6 condensates are relevant. The dimension-4 condensate $\langle \mathcal{O}_4 \rangle$ accounts for one parameter since it is chiral-invariant $\langle \mathcal{O}_4 \rangle \equiv \langle \mathcal{O}_4 \rangle_V = \langle \mathcal{O}_4 \rangle_A$ and the dimension-6 condensates are chosen to satisfy the relation $\langle \mathcal{O}_6 \rangle_A = -\frac{11}{7} \langle \mathcal{O}_6 \rangle_V$, derived from factorization: this adds one more parameter. Figure 1 indicates approximately the favored region for $\langle \mathcal{O}_4 \rangle$ and $\langle \mathcal{O}_6 \rangle$, such that the RMS error can be below 9% for an appropriate value of l_1 . For this case, $n = 3$.

Inside this favored region, we picked the point denoted by B on the figure. The outputs for this Set B are given in Table I.

In Table I, we indicate the result for low-energy observables, without condensate (Set A) and with condensates (Set B). We remind the reader of the correspondance between our parameters and QCD condensates. We present the values of the six low-energy observables taken into account in the fit, as compared to the values extracted from [25]. We also give the corresponding predictions for the low-energy constants of χ PT, as compared to the $\mathcal{O}(p^4)$ fit of [26]⁵, renormalized at the scale $\mu = 770$ MeV. Note that the presence of positive $\langle \mathcal{O}_4 \rangle$ and $\langle \mathcal{O}_6 \rangle$ essentially improves the prediction for f_π and the L_i constants, as

⁴ This is because the decays mentioned involve the squares of the couplings appearing in the lagrangian: to treat the couplings we are interested in on the same footing as f_π, M_ρ, M_{a_1} (which appear squared in the lagrangian), we consider the fourth-root of the decays $\Gamma_{\rho \rightarrow ee}^{1/4}, \Gamma_{\rho \rightarrow \pi\pi}^{1/4}, \Gamma_{\tau \rightarrow a_1 \nu_\tau}^{1/4}$. It is on these six quantities that we expect the precision to be of the same order. Note that this procedure is very close to that of [2], except that we fit directly observables rather than couplings.

⁵ At the level we are working, it does not make sense to consider $\mathcal{O}(p^6)$ fits.

TABLE I: Results for the two cases: without and with condensates. The signs $\equiv X$ means that the corresponding input parameter is fixed to the value X .

	Set A	Set B	QCD	Unit
l_1	$\equiv 3.1$	$\equiv 3.1$	$\sim 1/\Lambda_{\text{QCD}}$	GeV^{-1}
$\langle \mathcal{O}_4 \rangle$	$\equiv 0$	$\equiv 0.5 \times 10^{-3}$	$\frac{1}{12\pi}\alpha_s \langle GG \rangle > 0$	GeV^4
$\langle \mathcal{O}_6 \rangle$	$\equiv 0$	$\equiv 0.7 \times 10^{-3}$	$\frac{28}{9}\pi\alpha_s \langle \bar{q}q \rangle^2 > 0$	GeV^6
f_π	72.6	84.3	92.4 ± 0.3	MeV
M_ρ	776	796	775.8 ± 0.5	MeV
M_{a_1}	1.24	1.34	1.230 ± 40	MeV
$\Gamma_{\rho \rightarrow ee}$	5.63	5.80	7.02 ± 0.11	KeV
$\Gamma_{\rho \rightarrow \pi\pi}$	160	124	150.3 ± 1.6	MeV
$\Gamma_{\tau \rightarrow a_1 \nu_\tau}$	0.563	0.580	0.414	meV
$10^3 L_1$	0.36	0.45	0.4 ± 0.3	
$10^3 L_2$	$0.73 (= 2L_1)$	$0.89 (= 2L_1)$	1.35 ± 0.3	
$10^3 L_3$	$-2.2 (= -6L_1)$	$-2.7 (= -6L_1)$	-3.5 ± 1.1	
$10^3 L_9$	4.7	5.5	6.9 ± 0.7	
$10^3 L_{10}$	$-4.7 (= -L_9)$	-5.4	-5.5 ± 0.7	

is readily seen from the approximate expressions of Appendix B. In summary, condensates improve the matching between very low energies (f_π and L_i 's of χPT) on one hand, and very high energies ($N_c = 3$) on the other hand.

B. Interpretation

In such a model of large- N_c QCD treated at leading order, we expect corrections in $1/N_c$ to parameters in the lagrangian. To facilitate comparison with [2], we have considered square root of such parameters here. Still, experience shows that large- N_c models usually fare better than this rough estimate, except for some observables in which disagreement is expected (an example here is $\Gamma_{a_1 \rightarrow \pi\gamma}$, see Appendix B, where the related case of $L_9 + L_{10}$ is also discussed).

Our benchmark Set A, with vanishing condensates, already has an RMS error of 12.5%. Still, our analysis indicates a preference for non-vanishing condensates: Set B has an RMS error of 8.5%. Fixing the best fit involves just low-energy quantities such as decays and masses, but from this set of observables one can infer information about the high energy. The output is that the preferred signs for the condensates agree with those predicted by QCD: $\langle \mathcal{O}_4 \rangle > 0$ and $\langle \mathcal{O}_6 \rangle > 0$. In fact, the absolute value of $\langle \mathcal{O}_4 \rangle$ is consistent with the values extracted from QCD phenomenology (see for instance [27, 28, 29], and references therein).

As for the dimension-6 condensate, we can estimate its size using factorization. However, since we have not explicitly introduced the quark masses and the strong coupling constant into the model, $\alpha_s \langle \bar{q}q \rangle^2$ can only be obtained from $m_q \langle \bar{q}q \rangle$ using input from QCD. One starts from the Gell-Mann-Oakes-Renner relation

(Eqs.(2.16-2.17)), giving a value of $m_q \langle \bar{q}q \rangle$. Using knowledge of the quark masses and including corrections, [30] finds $\langle \bar{q}q \rangle (2 \text{ GeV}) = (0.267 \pm 0.016 \text{ GeV})^3$. This yields $28/9\pi\alpha_s \langle \bar{q}q \rangle^2 \sim 10^{-3} \text{ GeV}^6$, with quite large errors that encompass our favored values of $\langle \mathcal{O}_6 \rangle$ (Table I and Figure 1). Note that phenomenological QCD studies (see for instance [31, 32, 33, 34, 35, 36, 37, 38] and references therein) find in general a larger value for the dimension-6 condensate, more difficult to reconcile with factorization.

Finally, note that the favored region we have found corresponds to an approximate cancellation between the effects of $\langle \mathcal{O}_4 \rangle$ and $\langle \mathcal{O}_6 \rangle$ on w_V , while they add up in the axial channel. This supports the success of the model of [2, 3], where condensates were introduced in the axial channel only, via a bulk scalar field.

IV. CONCLUSIONS

We have started from the simplest model of holographic QCD and described a way to implement term by term the OPE of QCD. The 5D model we start with is the simplest in the sense that it is defined in terms of Yang-Mills fields only, with appropriate BCs that implement the spontaneous symmetry-breaking. This model has only two free parameters: a scale given by the inverse of the extension of the extra dimension, and a parameter to be identified with the number of colors of QCD.

In AdS, distance in the extra dimension measures the 4D momentum: each condensate, giving an giving a power-correction in $1/Q^{2d}$ in the deep euclidean, corresponds in the 5D picture to a power-correction z^{2d} to the AdS metric, where z measures the separation from the UV brane. We use a formalism involving a spurion, equivalent to considering two different metrics for the

vector and axial fields. This describes order parameters in the QCD language.

The expansion in modifications of the metric is under control. First, we find that the naive estimate for its size is indeed verified by data and secondly, the effect of these modifications become irrelevant as the dimension of the condensate increases. This justifies a posteriori our procedure of including deformations of the metric rather than higher-order operators.

By introducing the modifications of the metric, we show that the infinite number of Weinberg sum rules are reduced to the desired number, i.e. two. Also note that the high-energy properties of the amplitudes studied in [4] are not lost, and in fact, a similar property for the axial form factor can be demonstrated.

In terms of input parameters, this model with condensates adds two: the dimension 4 and 6 condensates $\langle \mathcal{O}_4 \rangle_V = \langle \mathcal{O}_4 \rangle_A$ and $\langle \mathcal{O}_6 \rangle_V = -7/11 \langle \mathcal{O}_6 \rangle_A$. We performed a complete numerical analysis of the effect of those condensates on hadronic observables: $f_\pi, M_\rho, M_{a_1}, \Gamma_{\rho \rightarrow e e}, \Gamma_{\rho \rightarrow \pi \pi}^{1/4}$ and $\Gamma_{\tau \rightarrow a_1 \nu \tau}^{1/4}$. We find that the presence of the condensates improves the agreement from 12.5 % to 8.5 %, even though the number of parameters has increased from 1 to 3. Moreover, the favored region in the parameter space corresponds to non-zero values for both dimension 4 and 6 condensates. The specific value for $\langle \mathcal{O}_4 \rangle$, corresponding to $1/(12\pi)\alpha_s \langle G_{\mu\nu} G^{\mu\nu} \rangle$, is of $(0.2 \div 0.8) \times 10^{-3} \text{ GeV}^4$. For $\langle \mathcal{O}_6 \rangle$, corresponding to $28/9\pi\alpha_s \langle \bar{q}q \rangle^2$, the preferred range is $(0.4 \div 1.0) \times 10^{-3} \text{ GeV}^6$, in agreement with the signs and orders of magnitude expected from QCD and factorization for the dimension-6 condensate.

We also extracted the corresponding low-energy constants: condensates improve the agreement. In particular, both $L_9 + L_{10}$ and $\Gamma_{a_1 \rightarrow \pi \gamma}$ become non-zero, in connection with the presence of a dimension-6 condensate. However, if factorization is not largely violated, both quantities remain smaller than the experimental value.

Apart from the already mentioned differences between our model and the one by [2, 3], we mention a more theoretical one: in the case of [2, 3], the massless pion is an admixture containing a bulk scalar, not protected by the gauge symmetry. In their construction, the limit of vanishing *condensates* implies the restoration of chiral symmetry in the spectrum: equal masses for the vector and axial resonances, and the absence of a massless pseudo-scalar. In our case, vanishing of *local* order parameters does *not* imply vanishing of *non-local* order parameters, and therefore chiral symmetry is still broken (the axial masses are distinct from the vector ones and the Goldstone bosons remain in the spectrum, with $f_\pi \neq 0$, see Appendix B). The only way to reinstate chiral symmetry in the spectrum is then to send f_π to zero. In practice, this requires $l_1 \rightarrow \infty$, i.e. the vanishing of the mass gap: a continuum of states is recovered. The converse of this statement, namely that confinement implies chiral symmetry breaking, is therefore built into our model.

Acknowledgments

We thank Leandro da Rold, Ami Katz, Toni Pich, Alex Pomarol, Jorge Portolés, Jan Stern and Pere Talavera for discussions. This work was partially supported by the Spanish MCyT grants BFM2002-00345 and FPA2004-00996, by the EC RTN networks MRTN-CT-2004-503369 and HPRN-CT-2002-00311 and by the Generalitat Valenciana grants GV04B-594, GV05/015, GV05/264 and GRUPOS03/013.

APPENDIX A: SYMMETRY-BREAKING, COVARIANCE AND LOCALITY

In the action (2.11), we introduced a term $\langle L_{MN} \Omega^\dagger R_{ST} \Omega \rangle$. It is clear that such a crossed term is going to affect the vector and axial channels differently, and thus introduce symmetry-breaking effects. The role of the auxiliary 5D field Ω is the following: one cannot simply write down $\langle L_{MN} R_{ST} \rangle$, because this term does not respect the 5D $SU(N_f) \times SU(N_f)$ group. To make it invariant, it appears that we need Wilson lines going from the point z to l_1 , but this would violate locality in the fifth dimension. This would be forgetting one thing: to make the whole procedure covariant, we should in addition reinstate the coset elements on the IR brane, which belong to the group $[SU(N_f) \times SU(N_f)] / SU(N_f)$ acting at $z = l_1$. The question is then the following: is there a way to write the appropriate combination of these elements as a local object?

The answer to the above turns out to be yes, as we show here. For simplicity, we start from the solution to the problem, and derive the result: we introduce an auxiliary field $\Omega(x, z)$ in the bulk, without kinetic term. Provided the right constraints are applied, this object can be decomposed as the above-mentioned product of Wilson lines and IR-brane coset elements. Therefore, a spurion Ω with a constraint solves the difficulty mentioned above, by allowing a writing that is both covariant and local. It is only by solving the constraint that the Wilson lines (and the coset element) appear. This we show below, as well as the rewriting in the form of two different metrics for (covariant) vector and axial combinations. As an intermediate step, we first reinstate the coset elements on the IR brane.

To do this, we go back to the question of symmetry breaking by BCs. Rather than directly identifying connections on the IR brane, we use a spurion on the IR brane to render the formalism covariant. This amounts to performing the identification up to a gauge, as done in [39]. In the present case, one would introduce a field $\omega(x)$ living on the IR brane, on which the constraint $D_\mu \omega = 0$ is applied. ω should in fact be an element of the coset of the transformations on the IR brane, i.e. it belongs to $[SU(N_f) \times SU(N_f)] / SU(N_f)$. In other words, it is unitary, and transform as a bi-fundamental under the $SU(N_f) \times SU(N_f)$ gauge group. We impose the two

constraints

$$\begin{aligned} 0 &= D_\mu \omega(x) \\ &= \partial_\mu \omega(x) - i R_\mu(x, l_1) \omega(x) + i \omega(x) L_\mu(x, l_1) \quad (A1) \\ 0 &= L_{5\mu}(x, l_1) + \omega^\dagger(x) R_{5\mu}(x, l_1) \omega(x), \quad (A2) \end{aligned}$$

which are both invariant under the 5D $SU(N_f) \times SU(N_f)$ gauge group. They provide a covariant replacement for the BCs on the IR brane.

This defines the model as well as BCs: one can then choose to gauge away the coset element ω , the rest of the algebra is then strictly identical to that of [4]. Alternatively, one may want to preserve covariance all along, in which case the definitions should be slightly modified: for instance, the rotations $\xi_{L,R}(x, z)$ appearing in the field redefinitions used to obtain appropriate vector and axial fields $\hat{V}_M, \hat{A}_M = \frac{i}{2} \left\{ \xi_L^\dagger (\partial_M - i L_M) \xi_L \pm \xi_L^\dagger (\partial_M - i L_M) \xi_L \right\}$ should involve Wilson lines, but also the field ω . The constraint to respect is that

$$\begin{aligned} \xi_R(x, z) \xi_L^\dagger(x, z) &= P \left\{ \exp \left(i \int_{l_1}^z dx^5 R_5(x, x^5) \right) \right\} \omega(x) \\ &\times P \left\{ \exp \left(i \int_z^{l_1} dx^5 L_5(x, x^5) \right) \right\} \quad (A3) \end{aligned}$$

With this definition, the matrix $U(x)$ collecting the pions is still written as $U = \xi_R(x, l_0) \xi_L^\dagger(x, l_0)$, and all equations follow identically as in [4], but now preserving the full covariance at each step.

This shows how a 4D spurion on the IR brane reintroduces the coset element necessary for a covariant description of the symmetry-breaking conditions at the boundary. Note that the original lagrangian was local, but our field redefinitions are non-local in the fifth dimension, since they involve Wilson lines: this will always be the case in such a model where the GB mode *is* the Wilson line, and therefore non-local. We now move to the question of the bulk auxiliary field $\Omega(x, z)$: we start from a local and covariant lagrangian generalizing the previous

idea. We have already mentioned the constraint to be imposed

$$\begin{aligned} 0 &= D_5 \Omega(x, z) \\ &= \partial_5 \Omega(x, z) - i R_5(x, z) \Omega(x, z) \\ &\quad + i \Omega(x, z) L_5(x, l_1), \quad (A4) \end{aligned}$$

as well as the BC for Ω

$$D_\mu \Omega(x, z = l_1) = 0, \quad (A5)$$

when we wrote down the action (2.11). Let us now describe how, starting from a lagrangian that respects locality in the fifth dimension, as well as covariance under the 5D $SU(N_f) \times SU(N_f)$ gauge group, the constraints above induce two different metrics for vector and axial field strengths.

The solution to the constraint (A4) can be written as

$$\begin{aligned} \Omega(x, z) &= P \left\{ \exp \left(i \int_{l_1}^z dx^5 R_5(x, x^5) \right) \right\} \Omega(x, l_1) \\ &\times P \left\{ \exp \left(i \int_z^{l_1} dx^5 L_5(x, x^5) \right) \right\}. \quad (A6) \end{aligned}$$

Using the BC (A5) then brings us back to the previous case, with the replacement $\omega(x) \mapsto \Omega(x, l_1)$, and all the equations follow. In particular, we see that

$$\begin{aligned} &(w_V(z) + w_A(z)) \langle L_{MS} L_{NT} + R_{MS} R_{NT} \rangle \\ &+ 2(w_V - w_A) \langle L_{MN} \Omega^\dagger R_{ST} \Omega \rangle \\ &= 4w_V \langle \hat{V}_{MN} \hat{V}_{ST} \rangle + 4w_A \langle \hat{A}_{MN} \hat{A}_{ST} \rangle, \quad (A7) \end{aligned}$$

confirming the interpretation that this term splits the two metrics, at the level of the (covariant) vector and axial combinations of fields. From here on, the extraction of the lagrangian in terms of the pions U and the KK modes V_n, A_n proceeds as in [4]. The pion field is defined again by $U(x) = \xi_R(x, l_0) \xi_L^\dagger(x, l_0)$, which is also equal to $\Omega(x, l_0)$, hence the straightforward identification for the quark mass terms of Section II D.

APPENDIX B: APPROXIMATE EXPRESSIONS

We give approximate expressions for some quantities, at linear order in the condensates. Using reduced values of the condensates $o_4 \equiv \langle \mathcal{O}_4 \rangle / (N_c l_1^{-4})$ and $o_6 \equiv \langle \mathcal{O}_6 \rangle / (N_c l_1^{-6})$, we have ⁶

$$f_\pi = \frac{\sqrt{N_c}}{\sqrt{6}\pi l_1} \left(1 + \frac{3\pi^2}{8} o_4 + \frac{55\pi^2}{896} o_6 \right) + \mathcal{O}(o^2), \quad (\text{B1})$$

$$M_\rho \simeq \frac{2.40}{l_1} (1 - 3.35 o_4 + 0.38 o_6) + \mathcal{O}(o^2), \quad (\text{B2})$$

$$M_{a_1} \simeq \frac{3.83}{l_1} (1 + 1.01 o_4 + 0.29 o_6) + \mathcal{O}(o^2), \quad (\text{B3})$$

$$L_3 = -3L_2 = -6L_1 = -\frac{11N_c}{1536\pi^2} \left(1 + \frac{3\pi^2}{2} o_4 + \frac{145\pi^2}{8624} o_6 \right) + \mathcal{O}(o^2), \quad (\text{B4})$$

$$L_9 = \frac{N_c}{64\pi^2} \left(1 + \frac{25\pi^2}{24} o_4 + \frac{5\pi^2}{448} o_6 \right) + \mathcal{O}(o^2), \quad (\text{B5})$$

$$L_{10} = -\frac{N_c}{64\pi^2} \left(1 + \frac{25\pi^2}{24} o_4 - \frac{3\pi^2}{448} o_6 \right) + \mathcal{O}(o^2). \quad (\text{B6})$$

It turns out that the expressions are accurate to a few percent for the range of interest (the one of Figure 1).

Adding (B5) and (B6) shows that, if $\langle \mathcal{O}_6 \rangle$ is of the order of magnitude expected from factorization one obtains $L_9 + L_{10} \sim 2 \times 10^{-4}$, i.e. one order of magnitude below the experimental value. Similarly, the model underpredicts the decay $\Gamma_{a_1 \rightarrow \pi\gamma}$ if factorization is respected. This can be understood as follows: a model that reproduces the width $\Gamma_{\tau \rightarrow a_1 \nu_\tau}$ has $f_{A_1} \sim 0.13$. Assuming that

⁶ The numerical coefficients stem from integrals of Bessel functions.

the sum rule (2.13) is saturated by the a_1 one can estimate $\Gamma_{a_1 \rightarrow \pi\gamma}$ from the knowledge of $L_9 + L_{10}$ from factorization. A suppression by an order of magnitude for $L_9 + L_{10}$ yields a suppression by two orders of magnitude for $\Gamma_{a_1 \rightarrow \pi\gamma}$. Indeed, we find that $\Gamma_{a_1 \rightarrow \pi\gamma} \sim \text{few keV}$ for the favored region of Figure 1, whereas experimentally one has $\Gamma_{a_1 \rightarrow \pi\gamma} = 640 \pm 246 \text{ keV}$ [25].

-
- [1] D. T. Son and M. A. Stephanov, Phys. Rev. **D69**, 065020 (2004), hep-ph/0304182.
 - [2] J. Erlich, E. Katz, D. T. Son, and M. A. Stephanov (2005), hep-ph/0501128.
 - [3] L. Da Rold and A. Pomarol, Nucl. Phys. **B721**, 79 (2005), hep-ph/0501218.
 - [4] J. Hirn and V. Sanz, JHEP **12**, 030 (2005), hep-ph/0507049.
 - [5] T. Sakai and S. Sugimoto (2005), hep-th/0507073.
 - [6] A. Karch and E. Katz, JHEP **06**, 043 (2002), hep-th/0205236.
 - [7] M. Kruczenski, D. Mateos, R. C. Myers, and D. J. Winters, JHEP **05**, 041 (2004), hep-th/0311270.
 - [8] M. Kruczenski, D. Mateos, R. C. Myers, and D. J. Winters, JHEP **07**, 049 (2003), hep-th/0304032.
 - [9] J. Babington, J. Erdmenger, N. J. Evans, Z. Guralnik, and I. Kirsch, Phys. Rev. **D69**, 066007 (2004), hep-th/0306018.
 - [10] N. J. Evans and J. P. Shock, Phys. Rev. **D70**, 046002 (2004), hep-th/0403279.
 - [11] C. Nunez, A. Paredes, and A. V. Ramallo, JHEP **12**, 024 (2003), hep-th/0311201.
 - [12] T. Sakai and S. Sugimoto, Prog. Theor. Phys. **113**, 843 (2005), hep-th/0412141.
 - [13] G. F. de Teramond and S. J. Brodsky, Phys. Rev. Lett. **94**, 201601 (2005), hep-th/0501022.
 - [14] N. Arkani-Hamed, A. G. Cohen, and H. Georgi, Phys. Rev. Lett. **86**, 4757 (2001), hep-th/0104005.
 - [15] J. Hirn and V. Sanz (2005), hep-ph/0510023.
 - [16] E. Witten, Adv. Theor. Math. Phys. **2**, 253 (1998), hep-th/9802150.
 - [17] S. S. Gubser, I. R. Klebanov, and A. M. Polyakov, Phys. Lett. **B428**, 105 (1998), hep-th/9802109.
 - [18] M. A. Shifman, A. I. Vainshtein, and V. I. Zakharov, Nucl. Phys. **B147**, 385 (1979).
 - [19] J. M. Maldacena, Adv. Theor. Math. Phys. **2**, 231 (1998), hep-th/9711200.
 - [20] N. Arkani-Hamed, M. Porrati, and L. Randall, JHEP **08**, 017 (2001), hep-th/0012148.
 - [21] E. Witten, Phys. Rev. Lett. **51**, 2351 (1983).
 - [22] J. Prades, Z. Phys. **C63**, 491 (1994), hep-ph/9302246.
 - [23] M. Knecht and A. Nyffeler, Eur. Phys. J. **C21**, 659 (2001), hep-ph/0106034.
 - [24] J. Gasser and H. Leutwyler, Nucl. Phys. **B250**, 465 (1985).
 - [25] S. Eidelman et al. (Particle Data Group), Phys. Lett. **B592**, 1 (2004), <http://pdg.lbl.gov/>.
 - [26] J. Bijnens, G. Ecker, and J. Gasser, in [?], hep-ph/9411232.
 - [27] F. J. Yndurain, Phys. Rept. **320**, 287 (1999), hep-

- ph/9903457.
- [28] B. L. Ioffe and K. N. Zyablyuk, Eur. Phys. J. **C27**, 229 (2003), hep-ph/0207183.
 - [29] M. Davier, A. Hocker, and Z. Zhang (2005), hep-ph/0507078.
 - [30] M. Jamin, Phys. Lett. **B538**, 71 (2002), hep-ph/0201174.
 - [31] M. Davier, L. Girlanda, A. Hocker, and J. Stern, Phys. Rev. **D58**, 096014 (1998), hep-ph/9802447.
 - [32] B. L. Ioffe and K. N. Zyablyuk, Nucl. Phys. **A687**, 437 (2001), hep-ph/0010089.
 - [33] V. Cirigliano, E. Golowich, and K. Maltman, Phys. Rev. **D68**, 054013 (2003), hep-ph/0305118.
 - [34] J. Rojo and J. I. Latorre, JHEP **01**, 055 (2004), hep-ph/0401047.
 - [35] K. N. Zyablyuk, Eur. Phys. J. **C38**, 215 (2004), hep-ph/0404230.
 - [36] S. Friot, D. Greynat, and E. de Rafael, JHEP **10**, 043 (2004), hep-ph/0408281.
 - [37] S. Narison, Phys. Lett. **B624**, 223 (2005), hep-ph/0412152.
 - [38] J. Bordes, C. A. Dominguez, J. Penarrocha, and K. Schilcher (2005), hep-ph/0511293.
 - [39] J. Hirn and J. Stern (2005), hep-ph/0504277.